

Design, Layout, and Testing of a Printed Circuit Board for Cyclic Voltammetry

By  
Karen Harper

A THESIS

submitted to

Oregon State University

University Honors College

in partial fulfillment of  
the requirements for the  
degree of

Honors Baccalaureate of Science in Electrical and Computer Engineering  
(Honors Scholar)

Presented June 7, 2019  
Commencement June 2019



## AN ABSTRACT OF THE THESIS OF

Karen Harper for the degree of Honors Baccalaureate of Science in Electrical and Computer Engineering presented on June 7, 2019. Title: Design, Layout, and Testing of a Printed Circuit Board for Cyclic Voltammetry

Abstract approved:

---

Matthew Johnston

This project concerns the design, layout, assembly, debugging, and testing of a Printed Circuit Board (PCB) that autonomously, reliably, and effectively conducts Cyclic Voltammetry (CV) measurements. CV is an electrochemical procedure done to analyze, quantize, and visualize reversible reduction-oxidation reactions, often used in medical devices to monitor the levels of certain hormones or other chemicals present in a persons body. As such, this PCB is meant to be portable and easy to use: the system is small, lightweight, and low-power, with a way to easily conduct these reactions, record the data, and send it to a phone or other external computer for processing and visualization. These actions all take place automatically, with no request from the user. This project was based on an existing PCB and uses the same microcontroller, Analog Front End chip, and Analog-to-Digital converter, but optimizes the voltage regulation, adds a battery charger and monitoring loop, and minimizes the Bluetooth antenna circuit. After the basic CV curve is obtained and analyzed through this new system, the parameters that affect a clean and presentable CV curve are noted and discussed. The board was tested using Ag/Ag<sup>+</sup> electrodes as the anode and 0.1M Ferrocenemethanol solution as the cathodic solution, and the results are compared to existing literature and to CV curves made by more precise desktop instruments.

Key Words: Cyclic Voltammetry, PCB, Redox, Design, Testing

Corresponding e-mail address: [harpekar@oregonstate.edu](mailto:harpekar@oregonstate.edu)

©Copyright by Karen Harper  
June 7, 2019  
All Rights Reserved

Design, Layout, and Testing of a Printed Circuit Board for Cyclic Voltammetry

By  
Karen Harper

A THESIS

submitted to

Oregon State University

University Honors College

in partial fulfillment of  
the requirements for the  
degree of

Honors Baccalaureate of Science in Electrical and Computer Engineering  
(Honors Scholar)

Presented June 7, 2019  
Commencement June 2019

Honors Baccalaureate of Science in Electrical and Computer Engineering project of  
Karen Harper presented on June 7, 2019

APPROVED:

---

Matthew Johnston, Mentor, representing Electrical and Computer Engineering

---

Matthew Shuman, Committee Member, representing Electrical and Computer  
Engineering

---

Jacob Dawes, Committee Member, representing Electrical and Computer  
Engineering

---

Toni Doolen, Dean, Oregon State University Honors College

I understand that my project will become part of the permanent collection of  
Oregon State University Honors College. My signature below authorizes release of  
my project to any reader upon request.

---

Karen Harper, Author

# Contents

<b>1</b>	<b>Acknowledgements</b>	<b>10</b>
<b>2</b>	<b>Abbreviations</b>	<b>11</b>
<b>3</b>	<b>Introduction</b>	<b>12</b>
<b>4</b>	<b>Project Specifications</b>	<b>13</b>
<b>5</b>	<b>Background Research</b>	<b>15</b>
5.1	Electrochemical Background . . . . .	15
5.2	Applications for CV Testing . . . . .	19
<b>6</b>	<b>Theory, Design, and Fabrication</b>	<b>21</b>
6.1	Relevant Other Projects . . . . .	21
6.2	PCB Design . . . . .	23
<b>7</b>	<b>Setup &amp; Results</b>	<b>24</b>
7.1	After-Fab PCB Revisions . . . . .	24
7.2	Data Collection and Analysis workflow . . . . .	27
7.3	Output Waveforms . . . . .	27
<b>8</b>	<b>Conclusion</b>	<b>30</b>
8.1	Project Discussion . . . . .	30
8.2	Further Research . . . . .	31
<b>9</b>	<b>Appendix</b>	<b>33</b>
9.1	Schematics . . . . .	33
9.2	Software Samples . . . . .	34
9.2.1	Microcontroller C: Representative Functionality only with Li- braries Omitted . . . . .	34



<i>CONTENTS</i>	9
9.2.2 MATLAB For Data Analysis and Presentation . . . . .	38
<b>10 References</b>	<b>39</b>

# 1 Acknowledgements

Thank you to Dr. Matthew Johnston, my thesis mentor, for use of his lab, help with project design and planning, and general support through the entire thesis process

Thank you to Jacob Dawes, a Ph.D. student in Dr. Johnstons lab, for providing the initial board designs, providing design reviews, and help with software development. He was also on my Thesis Defense Committee.

Thank you to Dr. Roger Traylor, a professor of ECE at Oregon State who wrote the TWI\_master library that I used.

Thank you to Matthew Shuman, an instructor of ECE at Oregon State who was on my Thesis Defense Committee.

Thank you to Aaron Schraner, who helped with the analog sweep circuit and software

Thank you to my family, for their never-ending love and support throughout my entire undergraduate career

## 2 Abbreviations

**ADC:** Analog to Digital Converter

**AFE:** Analog Front End. The part of a mixed-signal system that takes in analog signals and distributes them to other functions—in this case, the AFE board is the LMP91002.

**CV:** Cyclic Voltammetry. The way of visualizing and characterizing reversible redox reactions that this project was designed to accomplish.

**IC:** Integrated Circuit. A chip that contains some amount of specified circuit functionality in a small space.

**ISP:** In-System Programming. A type of microcontroller-to-computer communication often used instead of a USB interface to program the microcontroller

**PCB:** Printed Circuit Board

**QD:** Quantum Dot. A specific type of semiconductive material that CV was used to characterize.

**USB:** Universal Serial Bus. A common type of serial connector.

### 3 Introduction

This project concerns the creation, testing, and implementation of a Printed Circuit Board to conduct simple CV experiments. Optimally, the board will perform well enough that upon completion this PCB will be able to be further utilized by Dr. Johnstons and other labs around campus. As CV is often used in biological and medical applications, the emphasis will be for the PCB to be as small, low-power, and easy to use as possible—theoretically, with the idea that it could be functionally used as a wearable medical device.

CV tests include cycling a voltage potential across a reduction-oxidation (redox) type chemical reaction and measuring the charge that is transferred, and therefore current reduced, as a result of that applied voltage. In this specific application, the redox reaction is required to be cyclical or reversible, so any reaction that occurs with a potential sweep in a direction can be reversed if the applied potential is swept back the opposite direction. This is what causes the characteristic Duck Curve of cyclic voltammetry, shown in Figure 1. The potential values for the cycles beginning and end, what the current maxima and minima are and what voltage value they occur at, and the saturation current values on either side of the voltammogram all represent important characteristics of a specific cyclic voltammetry experiment and all must be recorded and understood in order to correctly characterize a system.

Most implementations of a CV instrument utilize a Potentiostat circuit, shown in Figure 2. The Counter, Working, and Reference Electrodes are usually arranged on a single test strip for compactness and ease of use, and the circuit itself allows for easy monitoring of the applied potential as well as the current it excites. However, despite the relatively compact nature of the electrodes, the precision required in making proper lab-grade measurements has historically required Potentiostat hardware to be large, expensive, and bulky. One of the only products currently on the market

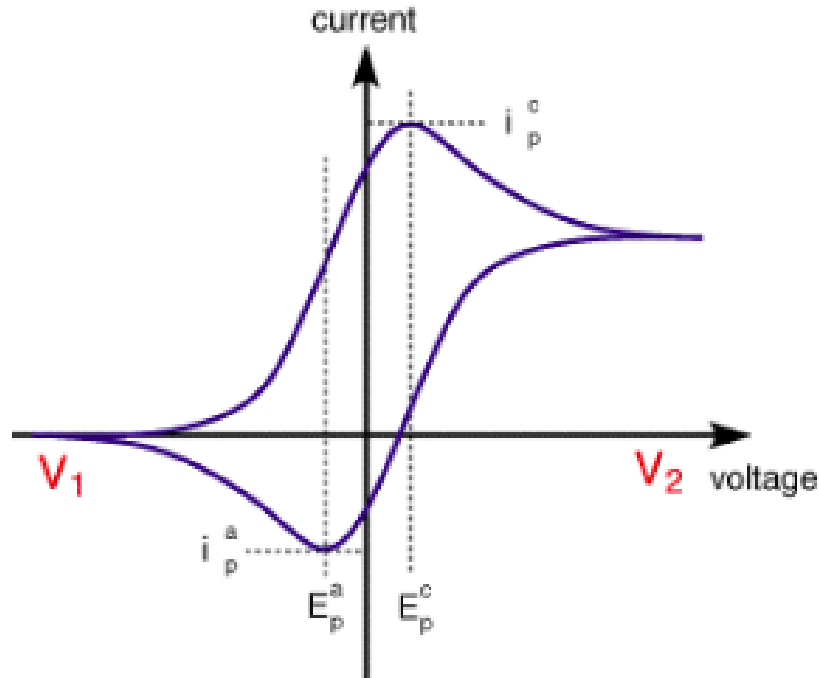


Figure 1: A Basic CV Curve

at the moment that specifically implements potentiostat functionality is the Epsilon EClipse, which costs \$6500 just for the potentiostat itself and another \$950 for the required software and \$3150-\$5985 for additional supporting hardware [3]. This may well be necessary for some projects and measurements, but if a small, low-cost, and low-power version of that circuitry could be designed to do a reasonable approximation of those measurements, then that could make it more accessible and available to people with neither the finances nor the motivation to maintain such a large and complicated test system. This is the line of logic upon which this project was based.

## 4 Project Specifications

This project aimed to be as small, lightweight, and low-power as possible, as the theoretical application of this technology would be a medical device or something else

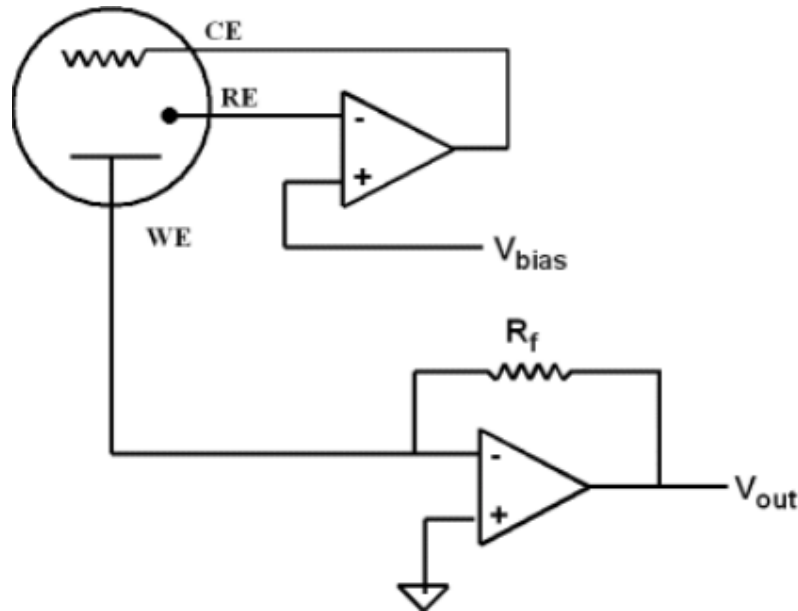


Figure 2: A Standard Potentiostat Circuit

that is always carried on someones person. A first version of this board existed in this lab previously, but it was relatively basic: it had only the LMP91002 AFE chip, an ADC, and a Bluetooth antenna so that the board could communicate with a laptop or other central machine to do data analysis and presentation. This first PCB version is shown in Figure 6, to be contrasted with the final layout of the second revision which is in Figure 14 in the Appendix.

This second version of the board was required to be equally as small as the first version or smaller, run on a standard size LiPo battery and preferably be independently rechargeable, have a battery monitor, and have a Nyquist filter between the 91002 chip and the AFE chip in order to block out some of the higher-frequency noise that will be injected into the system by the environment. The cyclic voltammetry functionality of the system was required to be as good or better as the first iteration, while it is running off of a LiPo battery instead of a coin cell, taking as little power as possible (the suggestion being with a switching power supply design), be programmed using an ISP header instead of a USB interface, and remaining lightweight

and portable. The software language to be used for the project was not specified, but since C was used for the embedded software development and MATLAB for the data processing and presentation in the first revision of the project, it was assumed that these would be maintained for ease of use and backwards compatibility.

## 5 Background Research

### 5.1 Electrochemical Background

Cyclic voltammetry is an application of electrochemistry, and more specifically a potentiostat, to monitor and quantify a reversible reduction-oxidation reaction. The circuit will cycle an applied potential between a designed high and low value, causing one of the reactants to oxidize and lose one electron/gain one charge while the other gains an electron/loses a charge. This forms what is commonly known as a reduction-oxidation or redox reaction, and if the oxidant and reactant can switch places after the reaction is done and the reaction can reverse, the electron can flow back from the original product to the original reactant and the process can start again. This doubling back process is what creates the characteristic duck curve of cyclic voltammetry, a theoretical representation of which is shown in Figure 1.

This procedure works, as all potentiostat circuits do, through a Counter electrode, Reference electrode, and Working electrode. The substance from which these are constructed depends on the solution that is to be measured during the experiment, but in general, the Working Electrode is made from a chemically inert substance while the Reference and Counter electrodes are the ones that actually carry out the reaction. These electrodes can be realized either as probes that are inserted into the solution of concern or as a specially designed test strip that has all three electrodes in a single package upon which chemical solution and electric potential is applied. As long as all three electrodes are interacting equally with the solution and free passage of charges

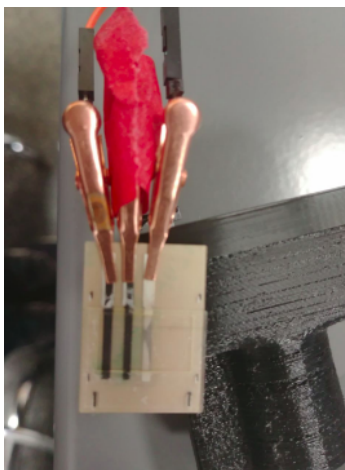


Figure 3: The Ag/AgCl electrode used for this project

is allowed among them, it does not strictly matter which experiment topography is used: the solution-and-probes experiment is more precise but requires more setup, more material available both of electrodes and of solution, and a potentiostat circuit capable of processing these larger voltage and current magnitudes that are caused by the increased reactant volume. The test strip setup is more compact and only requires a small bit of reactant, but the strips themselves are a bit nonstandard as test equipment and thus are a bit harder to find. Since the idea behind this project was that it should be as small as possible in order to fit the form factor of a wearable medical device, the test-strip setup with solution spread across the electrodes was used. A picture visualizing the electrode setup over the course of this project in in Figure 3.

After the experiment is properly set up with the three electrodes all making contact with the reactant in question, the actual CV measurement can begin. To carry out a CV measurement, a voltage that ramps from the  $V_1$  to the  $V_2$  in Figure 1 and back again is applied on the Reference electrode. This growing potential difference between the Reference electrode and the Internal Ground or Virtual Ground (Noted as  $V_{\text{bias}}$  in Figure 2, chosen internally on the LMP91002 IC) causes energy to flow



from the potentiostat op amp as an attempt to regulate that disparity. This forces current into the Counter Electrode, through the electrochemical cell created on the test strip, through the working electrode, and into the transimpedance amplifier to be translated from an output current into a voltage which can be more easily collected and reported by the system.

The magnitude of peak output current, values of input voltage for which the current output peaks, and symmetry of saturation voltages on the positive and negative ends of the hysteresis curve all contain important electrochemical information about the chemicals present in the reaction, their concentrations, and their relative reactivities with each other. The basic Duck Curve shape can be modeled with a basic Electrochemical equation known as the Nernst Equation:

$$E = E^0 + \frac{R * T}{F} * \ln\left(\frac{(Ox)}{(Red)}\right) \quad (1)$$

Where  $E^0$  is the standard potential of a reactant, which is the potential of a cell measured at standard conditions—all specie concentrations at 1M, all gas pressures at 1 atm, and temperature at  $25^\circ C$ . The (Ox) and (Red) values are the concentrations of the Oxidative and Reductive species, and R, T, and F are universal gas constant, Temperature, and Faradays constant, respectively [3].

So, the voltage starts at its highest point, at around  $V_1$  in Figure 1 or Point A in Figure 4 [3]. It is customary in the construction of a CV duck curve to start at the lower current value/higher voltage value and have the x-axis sweep up in order to have the ducks bill in the right side of the plot, as shown in Figure 4. As the voltage is swept negatively down towards point D, the charged oxidative ion is reduced down relatively linearly until point C, where the peak cathodic current lies. At this point, the volume of solution at the surface of the electrode is maximized, and transport of the oxidative ion is slowed which is what causes the decrease in current from point

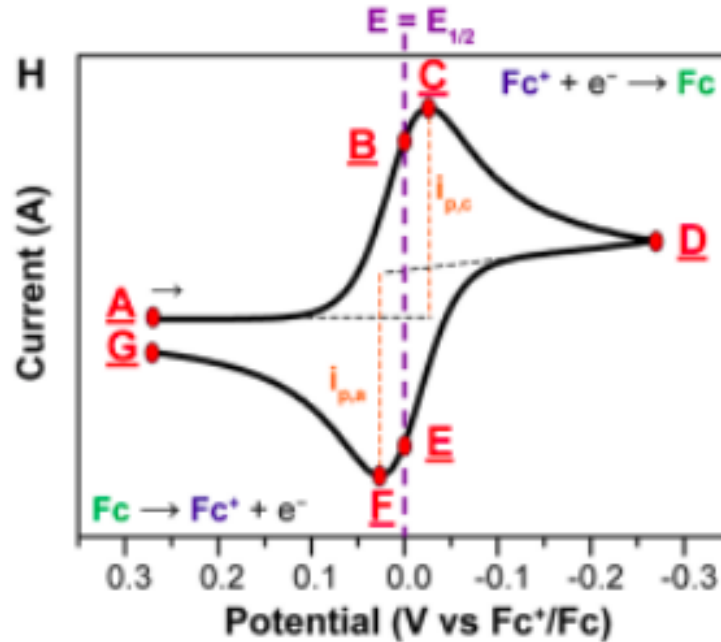


Figure 4: CV Curve with important points labeled

C to Point D. The same process, albeit with a reversed applied potential, follows the re-oxidation of the ion through points E, F, and G [3].

A crucial factor in a CV experiment is the scan rate—faster scan rates lead to quicker decreases in the diffusion layer, so higher currents are observed as a result. If a reaction is fully electrochemically reversible and involves freely diffusing species, the peak current can be described using the Randles-Sevcik equation [3]:

$$i_p = 0.446 * n * F * A * C^0 * \left( \frac{n * F * v * D_0}{R * T} \right)^{\frac{1}{2}} \quad (2)$$

Where  $n$  is the number of electrons passed around during the reaction (sometimes known as the order of the electrochemical reaction),  $v$  is the scan rate,  $F$  is Faradays constant, and  $C^0$  is the bulk concentration of the analyte.  $D_0$  is called the diffusion coefficient of the oxidized analyte, and it describes the maximum amount of material that can be diffused for a certain period of time. It is measured in  $\frac{m^2}{s}$ . [3]

CV and electrochemistry in general can quickly get very specific—lots of work is done to ensure that any one specific curve has its peaks at the right places and at the right magnitudes, and that the slope of the oxidation and reduction match up well with the theory. However, if Points C and F from Figure 4 are not at the midpoint of the plot and if the peaks are enough that the plot looks non-linear, those two points are enough to consider the plot non-linear and at least somewhat electrochemical in nature. [1]

## 5.2 Applications for CV Testing

CV is commonly used to succinctly relate information about a chemical reaction and the species involved in it. As it can effectively be used to represent virtually any reaction that contains two chemical species that can pass at least one change back and forth, and each individual test is relatively fast and easy to conduct once it has been set up and calibrated, CV is one of the most commonly used electrochemical tests done in laboratories. [1]

Many existing applications of CV especially on industrial scales are medical in nature. This is a result of the large number of macromolecules in the human body that transmit information from one place to another through the transmission of charge. It has been involved in the characterization of the bioactive organic compound xanthone, which was proved to be effective as a scavenger molecule for other reactive species, it proved that the antibiotic amoxicillin changes its redox behavior under exposure to metallic ions and amino acids, and it has played a crucial part in the design process of several biosensors as it can help quantify the change in reaction behavior due to diffusion, absorption of pollutants, and parasitic capacitance between the electrochemical cell and other nearby electronics. CV was even used to monitor the degradation of ibuprofen in different types of electrodes and used to simulate

the degradation pattern of this crucial drug in the human stomach [4]. Clearly, this process is well-known, relatively simple to use, and can give powerful and useful data about a reversible redox electrochemical reaction that can greatly benefit the scientists doing these tests and making these measurements.

However, CV can also be used for characterizing non-medical systems as well, just with a swapping out of electrode materials in order to ensure that the working electrode remains inert throughout the process. Since a large part of the CV curve is due to the movement of free electrons throughout the solution as the potential rises, a drastic change in the shape of the duck curve for a specific reaction can be due to an abnormality or impurity in the material being tested. In this way, the concentration of a desired reagent versus the concentration of an undesired or unwanted reagent can be determined, and the materials suitability for its intended application can be understood based on that objective data. As CV works on the scale of individual electrons moving back and forth between different molecules, it is even a good fit to work on the quantum scale: several studies have had success using it to calculate the Highest Occupied and Lowest Unoccupied Molecular Orbital values of some new organic semiconductors, and it has also proved useful in characterizing the behavior of the new Quantum Dot inorganic semi-conductive particles and aiding in the analysis of their stability in solution as research into them continues. Figure 5 shows the output CV curve of 0.1 M PBS electrolyte with 5 mM FcMeOH at different scan rates—this proves, in part, that the QDs show homogenous ion transport behavior and that they can be successfully manipulated into exchanging electrons with a Glassy Carbon electrode without losing too much stability. [5]

These are just some of the many examples of CV either participating or having the potential to participate in revolutionary chemical, physical, and engineering applications. It has also proven capable of participating in testing the optimal chemical

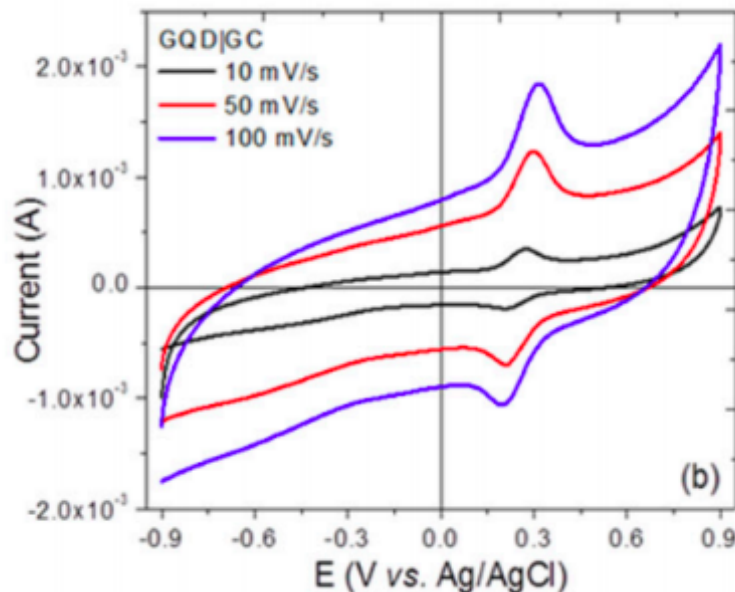


Figure 5: CV curves at different scan rates of a Quantum Dot

compound for different colors of paint, evaluating the stability and capability of potential new battery technologies, and even helped monitor a winemaking lab to make sure fermentation is happening correctly [4]. CV is an incredibly versatile and multidisciplinary testing procedure that has already provided crucial information about reactions in a large number of areas and will only become more prevalent as DSP functionality becomes more accessible in smaller areas and the technique becomes more well known.

## 6 Theory, Design, and Fabrication

### 6.1 Relevant Other Projects

As was mentioned previously, this PCB is a second revision of a PCB designed by Jacob Dawes. This PCB was successful in conducting a CV measurement, but its

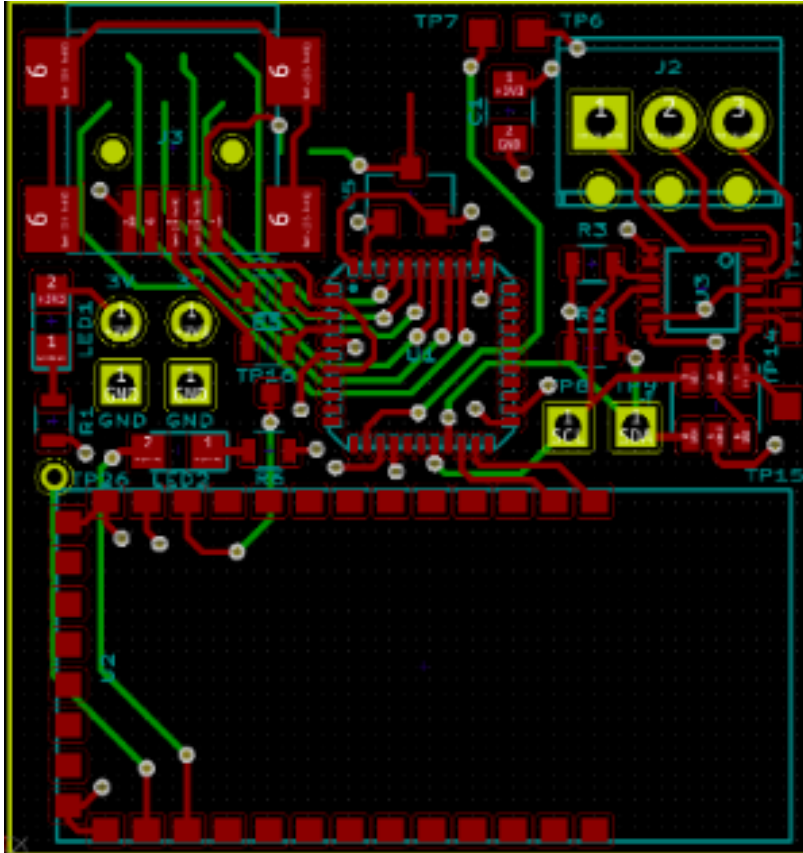


Figure 6: Revision 1 of the CV Board

voltage range was limited, it relied on programming over USB rather than an ISP header, and it used a separate board for its Bluetooth connection that had to be separately soldered on. It was also requested during there be a Nyquist filter between the LMP91002 IC and the ADC, so that some of the higher-frequency noise that is coupled in from having the system be so compact can be filtered out and the ADC reading can be more accurate. More robust power and battery management components were also suggested, such as a Battery charger, a Battery charge monitor, and a small switching power supply. The PCB completed for this project is based off of the same PCB form factor and some of the same component placements—an image of the KiCad model for this Revision 1 PCB is shown in Figure 6.

Another project which was some of the inspiration for and has a lot of the same goals as this Thesis project is that of the Masters Thesis of Wei Te, an Electrical Engineer from the Imperial College of London. The title of his Masters Thesis is A mini-PCB for Glucose-sensor readout and diagnostics, and in it he not only conducts CV testing on a compact, lightweight board, he also uses an AFE IC in the same family as the one used in this project (LMP91000 as opposed to LMP91002), very close to the same ADC, a similar bluetooth module, and a similarly-appearing test strip. However, this paper did not perform a CV sweep using the board designed during the project, instead using the circuit prototyped on a breadboard. The sweep was also performed on a resistor in lieu of an actual reversible redox reaction, which made the doubling back and proving the non-linearity of the oxidative sweep as opposed to the reductive sweep unnecessary.

## 6.2 PCB Design

The PCB was designed using KiCad EDA design suite, where it has 4 layers and is 31.57mm by 29.5mm. The detailed schematics can be found in the Appendix. The majority of the schematic was taken from application circuits on the datasheets for the respective chips, with the exception of the current-control resistor on the LED coming off of the ATmega, the design of the Reset button and its filtering capacitor as well as it being in parallel with the RESET pin from the power supply so either signal will reset the ATmega, and the Nyquist filter which was designed for 48Hz to optimize both transient time and filtering ability.

The PCB layout itself was relatively straightforward—the two internal layers were chosen for 3.3V and GND, and a design decision was made to put the majority of the components on one side in order to allow for easier assembly using a reflow oven. A Microstrip antenna was designed using Kicads Microwave Design tool, designed for a fourth-wavelength in FR-4 Board Material, and placed on the back of the board.

The decision was made to implement a Bluetooth module through discrete components instead of buying a separate PCB as a module and then needing to solder it on through headers or surface-mount pins onto the board, which would make the entire design less clean as well as taking up a large portion of one side of the board.

The Board was ordered from JLCPCB and the parts from Digikey, and both arrived in about a week. Though the board was specifically designed to allow for easier use of the reflow oven, it was later decided to use a Heat Gun and adhere each component on individually instead so as to compartmentalize problems and have an easier time with debugging. This unfortunately added time and made the final product look physically less clean than it would have otherwise, as it was essentially hand-soldered, but it was successful at fostering efficient debugging and produced an acceptable result.

## 7 Setup & Results

### 7.1 After-Fab PCB Revisions

After the PCBs came back from fabrication and after assembly and basic debugging started, it became clear that some additions and blue-wire changes were going to be necessary on the PCB to make it work as intended. The first and most obvious of which was that the pull-up resistor on the SDA line of the  $I^2C$  bus had not been correctly connected—the footprint was present on the PCB as it should have been, but there were no traces connecting it to the SDA and VCC lines. Once another resistor was blue-wired in so that this connection was made, the  $I^2C$  communication began to work as intended.

The most glaring and obvious post-fabrication edit, which required the addition of a protoboard-based daughter board, was the addition of an analog switch between the



original Galvanic cell output and where the output traces ended up being. This addition was required because there was a misunderstanding about what functionality the LMP91002 IC allowed for—it was assumed that it was able to cover all the necessary sweep potential by itself, but it was discovered after fabrication that it only allowed for four bits of resolution to set the input voltage to the cell, making the maximum applied potential 15mV. The new sweep circuit is shown in Figure 7, implemented on the board using BJTs because they were what was available at the time of these modifications. This new voltage sweep circuit makes use of the potentiostat amplifier some of the time by using it as an integrating amplifier, while an IO pin from the ATmega (also, for now, blue-wired) determines its direction and the switch determines whether the voltage is allowed to ramp or not. The software was modified to stop the ramping momentarily while a sample is being collected in order to avoid tainting of the data from changing the potential difference in the cell during measurement.

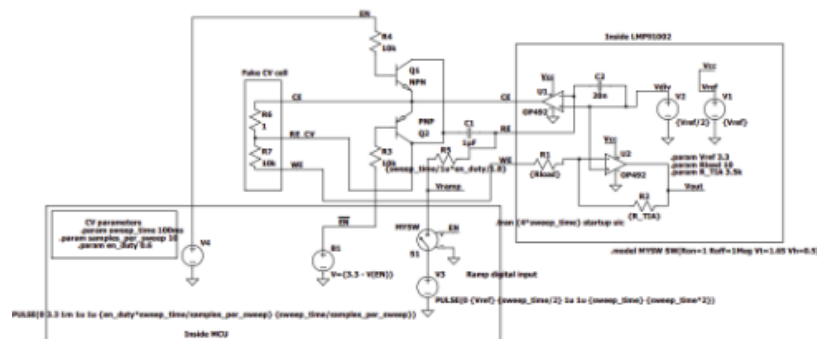


Figure 7: The new sweep circuit—everything in the box on the right is inside the LMP91002

It was also determined that the Reset Button and the chosen Switching Power Supply, MAX77596, had not been given the correct footprints. The Reset button only necessitated installing it at an angle to avoid perpetually shorting the nodes intended for connecting with a button press, but the footprint intended for the voltage

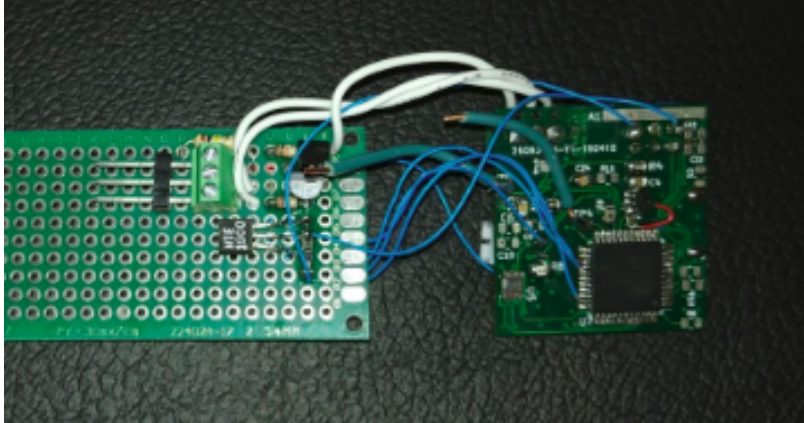


Figure 8: The Final Product with all after-fab edits

converter was deemed just small enough to be unusable by the intended IC. It was switched out with an NTE1900, which is not switching and also required a voltage divider to provide it with the correct voltage in order to operate correctly. With all these modifications and edits, the final product PCB is shown in Figure 8.

Though there were a relatively high number of issues with assembling this PCB, they would all be relatively easily solved with a second PCB revision now that they are all understood. A second PCB revision would allow the new ramp circuitry to be put onto the PCB itself, with the BJTs collapsing into an analog switch. The Enable and  $\overline{Enable}$  pins could also be turned into just one extra IO pin and an inverter, the SDA pull-up resistor could actually be connected to its proper nodes by default, and the footprint for the MAX77596 could be changed out with a slightly bigger one so that the IC could actually sit inside it. Those revisions would all be relatively simple and would allow for similar or better functionality with a much cleaner board form factor which is closer to what was originally intended.

## 7.2 Data Collection and Analysis workflow

Once ISP connection to the ATmega,  $I^2C$  connection to the AFE IC, UART capability from the ATmega, and a solid power supply connection were verified, a workflow was put in place in order to conduct CV tests, extract the data from the CV board and onto a laptop, and plot it in MATLAB to ensure the process is working correctly and that CV is actually being performed as it should. Once the ADC was confirmed to work as well it was incorporated into this workflow. The software for the functionality described below can be found in the Appendix.

Once the ATmega receives a reading from the ADC for the output voltage measurement at that moment and polls its internal ADC to determine what the value of the applied potential is, it concatenates these two measurements and sends them over UART. A Bus Pirate tool was used in conjunction with the source laptop to sniff these UART packets and convert them into a CSV, part of the initialization of which is shown in Figure 9. This CSV was then imported into MATLAB where data visualization was done, the software for which is also in the Appendix. It is mostly pretty classical read CSV and create a plot style software, the only somewhat unique part of which being that the sweep voltage for every sample has  $V_{CC}/2$  subtracted from it to renormalize it around the CV systems virtual ground and the ADC reading must be renormalized around virtual ground as well as being divided by the Transimpedance Amplifier resistor in order to convert that value back into current. This testing setup is shown in Figure 10, with the Bus Pirate connected to the UART Line, custom PCB connected to the computer via ISP, and connected to the test strip via the daughter board with the sweep circuit.

## 7.3 Output Waveforms

The first few CV tests were performed with only the AFE functional and not the ADC yet, so they are using the ADC on the Oscilloscope instead of the onboard one which

```
Stop bits:
 1. 1 *default
 2. 2
(1)>1
Receive polarity:
 1. Idle 1 *default
 2. Idle 0
(1)>
Select output type:
 1. Open drain (H=Hi-Z, L=GND)
 2. Normal (H=3.3V, L=GND)
(1)>1
Ready
UART>
```

Figure 9: Part of the initialization of a UART Channel from the Bus Pirate interface

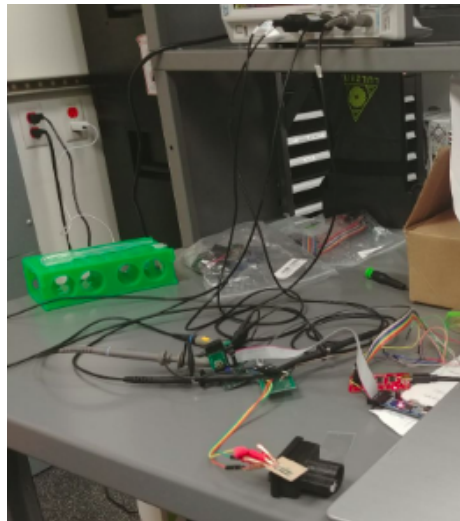


Figure 10: Testing Setup

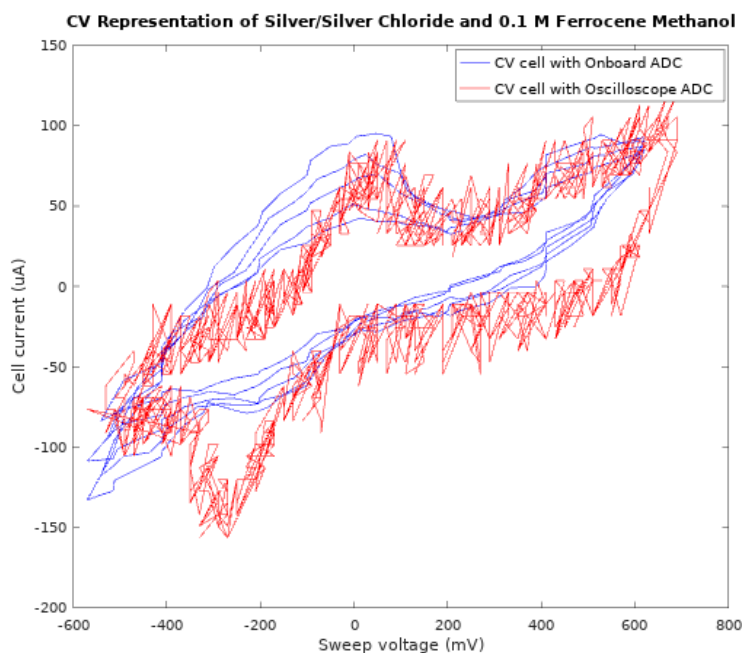


Figure 11: Output CV Measurements of the PCB and Project Workflow

has more bits. Though they are a little noisy and rough, they were enough to show the shape of the output CV curve from this project using 0.1M Ferrocenemethanol and Ag/AgCl electrodes—in Figure 11 below, the earlier data taken using the Oscilloscope ADC is shown in Red, and the later data taken using the onboard ADC is shown in Blue. There is an obvious and drastic difference in the size of the peak during the oxidative sweep between the ADC data and the Oscilloscope data, as well as a dip down by the left side of the plot where there once was a relatively flat tapering off, which is somewhat closer to the theory. It is likely that these two phenomena are connected, in that as the cell degraded from being used many times in a lossy chemical reaction, some of the material on the electrodes was physically displaced and was no longer useful.

Also of note is that the plot is not symmetrical—in both the earlier Oscilloscope plot and the later onboard ADC plot, the plot did not level and taper off on the

high potential side like one would expect when taking into account the low potential side and the CV theory, but rather it attained another high peak at right around the peak applied potential. This has a potential explanation in Figure 12: in the source material, that figure was meant to show how having too high of a sample rate can spread out the energy in a CV plot and marr the information within. It is possible that with a lower sample rate the plot would have looked slightly better on its right side. [4]

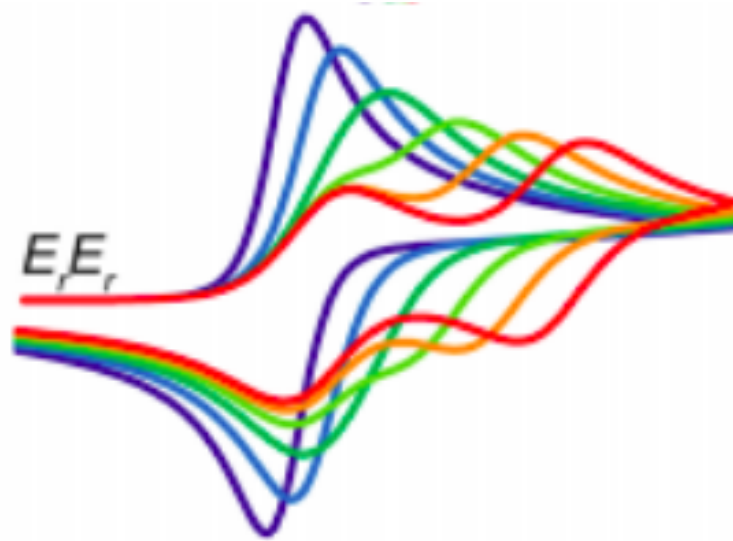


Figure 12: The effects of an increase in sample rate, with purple as lowest and red as highest

## 8 Conclusion

### 8.1 Project Discussion

Over the course of this project, a PCB has been designed, laid out, fabricated, assembled, tested, and been proven to work. CV curves were taken that matched up relatively closely with theory were taken, save for some discrepancies that were understandable and explainable when taking into account the degradation of the Galvanic

Cell, since those are usually supposed to be one-time or at least temporary-use items and the one for this project was run during testing about 20 or 25 times. It is also true that assembly was not fully completed—due to time constraints, the assembly of the Bluetooth module was not finished, and due to an incorrect footprint making assembly impossible, the MAX77596 buck converter was never soldered onto the board either. Nevertheless, the PCB was able to be programmed over ISP, the ATmega could program the ADC and the LMP91002 over  $I^2C$ , and the system could perform a CV sweep and output that data over UART, so all of the crucial functionality was there and worked reasonably well.

## 8.2 Further Research

While the initial results were encouraging, there are several relatively simple ways the performance of this PCB and project could be improved, as discussed above. In addition to simply making a second version of the board to fix all the footprint size and shape issues as well as integrating the voltage sweep circuit in a more compact way with inverters and an analog switch instead of discrete components, the voltage drop on the analog switch could be chosen to be lower than that on the BJTs used on this version, which meant that if all else went perfectly the system can only ramp from 0.7 to 2.6 V instead of closer to the voltage rails. There should also be more components on the back of the board—this was a design decision to allow for an easier time assembling this two-sided board in a reflow oven, but the assembly ended up taking place using a soldering iron and heat gun instead of a reflow oven, so this decision ended up just making one side of the board even more unnecessarily crowded than it needed to be.

It would also be good just for the robustness of the project and for more confidence in the results and what they mean to test the board both with more Ferrocenemethanol and Ag/AgCl electrodes, to ensure they also have relatively smooth

duck curves and that they begin to show degradation in the same ways this one is postulated to have done, and with more reversible redox reactions that center their responses at different applied potentials and have different output current magnitudes, to ensure that the response changes with respect to this as it is expected to. It would also be worthwhile to connect a battery for a long-term experiment and see how long it will last on one charge both in standby mode and constantly performing a CV sweep, as a medical device application would necessitate this information. These different experiments and changes to be made to the board will ensure that the resulting product looks, performs, and acts as a system in the most efficient way possible.





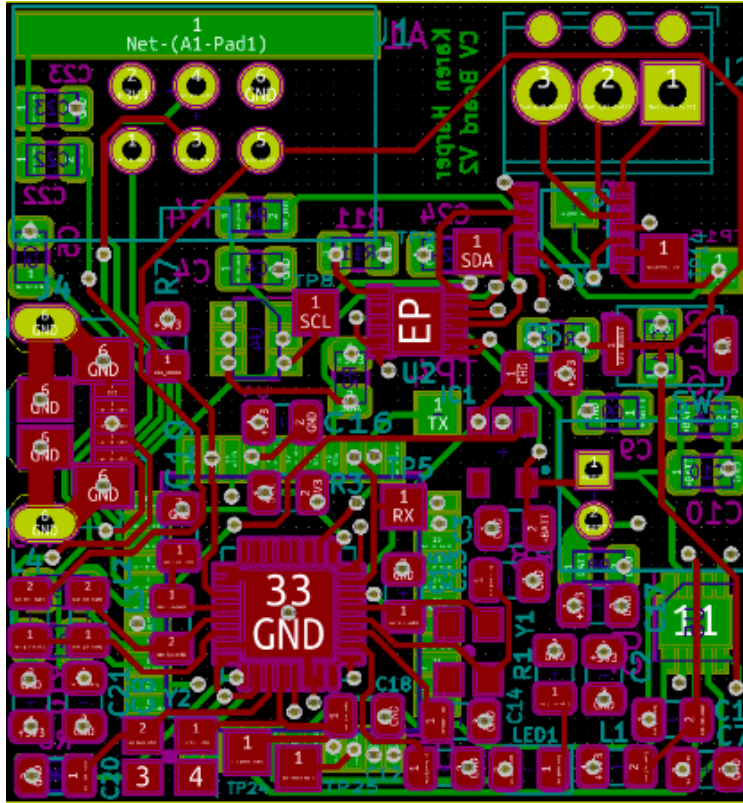


Figure 14: PCB Layout

## 9.2 Software Samples

### 9.2.1 Microcontroller C: Representative Functionality only with Libraries Omitted

```
#include <util/delay.h>
#include "twi_master.h"
#include "pin.h"
#include <unistd.h>
#include <util/twi.h>
#include <avr/interrupt.h>
#include "lmp.h"
#include "usart.h"
```

```
uint16_t cv_do_ramp(uint16_t* ramp_voltage_out, uint16_t* cv_current_out, uint16_t sa
    uint16_t sample_index = 0;
```

```
ramp_to_middle();

// ramp to bottom of sweep
while(read_int_adc() > RAMP_ADC_MIN) {
    ramp(RAMP_DOWN);
    _delay_ms(1);
}

// start taking CV measurements
// begin by ramping from min to max while taking samples
while(read_int_adc() < RAMP_ADC_MAX) {
    ramp(RAMP_UP);
    my_delay_ms(sample_period_ms - settling_delay_ms);

    // pause ramp for a few milliseconds so the voltage can settle
    ramp(RAMP_PAUSE);
    my_delay_ms(settling_delay_ms);

    // take sample
    if(sample_index >= max_samples)
        return sample_index;
    ramp_voltage_out[sample_index] = read_int_adc();
    cv_current_out[sample_index] = read_ext_adc();
    sample_index++;
}

// ramp back down and record CV measurements
while(read_int_adc() > RAMP_ADC_MIN) {
    ramp(RAMP_DOWN);
    my_delay_ms(sample_period_ms - settling_delay_ms);

    // pause ramp for a few milliseconds so the voltage can settle
    ramp(RAMP_PAUSE);
    my_delay_ms(settling_delay_ms);

    // take sample
    if(sample_index >= max_samples)
        return sample_index;
    ramp_voltage_out[sample_index] = read_int_adc();
    cv_current_out[sample_index] = read_ext_adc();
    sample_index++;
}
```

```
    }

    // return to midpoint
    ramp_to_middle();

    return sample_index;
}

int main() {
    init_twi();
    _delay_ms(100);

    // enable interrupts (required for TWI)
    sei();

    config_ext_adc();
    _delay_ms(10);

    config_int_adc();

    LMP my_lmp(LMP_ADDR_W);

    // unlock registers
    my_lmp.LOCK = LMP::LOCK_UNLOCKED;
    _delay_ms(10);

    //2.75kohm TIA gain
    my_lmp.TIACN = LMP::TIACN_2_75k;
    _delay_ms(10);

    //re-lock registers
    my_lmp.LOCK = LMP::LOCK_LOCKED;
    _delay_ms(10);

    // set operating mode to 3-lead amperometric cell with shorting FET turned off
    my_lmp.MODECN = LMP::MODECN_FET_NOSHORT | LMP::MODECN_OPMODE_AMPCELL;
    _delay_ms(10);

    uint16_t ramp_vin_samples[NUM_SAMPLES];
    uint16_t ramp_vout_samples[NUM_SAMPLES];
```

```

ramp_to_middle();
_delay_ms(500);
ramp(RAMP_DOWN);
while(read_int_adc() > 300) {
    _delay_ms(1);
    ramp(RAMP_PAUSE);
    _delay_ms(9);
    ramp(RAMP_DOWN);
}

while(1) {

    //int num_taken = cv_do_ramp(ramp_vin_samples, ramp_vout_samples, 100, NUM_
    for(int i=0; i<400 && read_int_adc() < RAMP_ADC_MAX; i++){
        ramp(RAMP_UP);
        _delay_ms(2);
        ramp(RAMP_PAUSE);
        _delay_ms(270); // settling time
        uint16_t int_adc = read_int_adc();
        uint16_t ext_adc = read_ext_adc();
        usart.print(int(int_adc));
        usart.print(", ");
        usart.print(ext_adc);
        usart.print("\r\n");
        _delay_ms(2);
    }

    for(int i=0; i<400 && read_int_adc() > RAMP_ADC_MIN; i++){
        ramp(RAMP_DOWN);
        _delay_ms(2);
        ramp(RAMP_PAUSE);
        _delay_ms(270); // settling time
        uint16_t int_adc = read_int_adc();
        uint16_t ext_adc = read_ext_adc();
        usart.print(int(int_adc));
        usart.print(", ");
        usart.print(int(ext_adc));
        usart.print("\r\n");
        _delay_ms(2);
    }
}
while(1);

```

```
}

```

## 9.2.2 MATLAB For Data Analysis and Presentation

```
function cv_adc (filename) #for using with the onboard ADC
    table = load(filename);
    int_adc = table(:,1);
    ext_adc = table(:,2);
    bits_int_adc = 10;
    bits_ext_adc = 15;

    R_tia = 2.75E3; # 2.75 kohm R_TIA
    sweep_voltage = (3.3 * int_adc / (2 ^ bits_int_adc - 1) - 1.65); # CV sweep voltage
    CV_current = -(3.3 * ext_adc / (2 ^ bits_ext_adc - 1) - 1.65) / R_tia; # CV current
    plot(sweep_voltage * 1000, CV_current * 1E6, 'b-')
    xlabel('Sweep voltage (mV)');
    ylabel('Cell current (uA)');
    title(filename)

endfunction

function cv (filename) #for using from the Oscilloscope ADC
    table = load(filename);
    ch_1 = table(:,1);
    ch_2 = table(:,2);

    R_tia = 2.75E3; # 2.75 kohm R_TIA
    sweep_voltage = ch_2 - 1.65; # CV sweep voltage
    CV_current = -(ch_1 - 1.65) / R_tia; # CV current
    plot(sweep_voltage * 1000, CV_current * 1E6, 'r-')
    xlabel('Sweep voltage (mV)');
    ylabel('Cell current (uA)');
    title("CV Representation of Silver/Silver Chloride and 0.1 M Ferrocene Methanol")
    legend("CV cell with Onboard ADC", "CV cell with Oscilloscope ADC")

endfunction
```

## 10 References

1. Chooto, P. (2019, January 28). Cyclic Voltammetry and Its Applications. Retrieved from <https://www.intechopen.com/online-first/cyclic-voltammetry-and-its-applications>
2. BASI Corporate Headquarters. (n.d.). Epsilon EClipse Quote Request. Retrieved June 1, 2019, from <https://www.basinc.com/products/ec/epsiloneclipse/quote>
3. Elgrishi, N. (2017, November 3). A Practical Beginners Guide to Cyclic Voltammetry. Retrieved March 15, 2019, from <https://pubs.acs.org/doi/pdf/10.1021/acs.jchemed.7b0036>
4. Te, W. K. (2017). A mini-PCB for Glucose-sensor readout and diagnostics. Imperial College London EEE4 Final Project. Retrieved May 4, 2019, from [https://sghoreish.github.io/Theses/Wei\\_Te.pdf](https://sghoreish.github.io/Theses/Wei_Te.pdf).
5. N/a. (n.d.). How the Potentiostat Works. Retrieved May 20, 2019, from <http://www.customsensorsolutions.com/ap-pstat.html> Cannes, C. (2002). Cyclic voltammetry and scanning electrochemical microscopy of ferrocenemethanol at monolayer and bilayer-modified gold electrodes. Retrieved May 30, 2019, from <http://bard.cm.utexas.edu/resources/Bard-Reprint/733.pdf>
6. Linear Sweep and Cyclic Voltammetry: The Principles. kla29@cam.ac.uk - <https://www.ceb.cam.ac.uk/Edu/linear-sweep-and-cyclic-voltammetry-the-principles>

